



Comparison study of phenol degradation using cobalt ferrite nanoparticles synthesized by hydrothermal and microwave methods

Leila Roshanfekar Rad^a, Babak Farshi Ghazani^b, Mohammad Irani^{b,*},
Mohammad Sadegh Sayyafan^c, Ismaeil Haririan^{d,e,*}

^aDepartment of Chemistry, Guilan Science and Research Branch, Islamic Azad University, Guilan, Iran, email: lrrchem@gmail.com

^bDepartment of Chemical Engineering, Amirkabir University of Technology (Tehran Polytechnic), Hafez Ave., P.O. Box 15875-4413, Tehran, Iran, email: farshi@aut.ac.ir (B. Farshi Ghazani), Tel. +98 021 22590926; Fax: +98 021 22600600; email: irani_mo@ut.ac.ir (M. Irani)

^cDepartment of Pharmaceutics, School of Pharmacy, Shiraz University of Medical Science, Shiraz, Iran, email: Sayyafanm@sums.ac.ir

^dMedical Biomaterials Research Center (MBRC), Tehran University of Medical Science, Tehran, Iran, email: haririan@tums.ac.ir

^eDepartment of Pharmaceutics, School of Pharmacy, Tehran University of Medical Sciences, Tehran, Iran

Received 4 April 2014; Accepted 14 September 2014

ABSTRACT

In the present study, the potential of synthesized cobalt ferrite nanoparticles using microwave (M-CF) and conventional hydrothermal (H-CF) methods for degradation of phenol was investigated during photo-Fenton-like process. The synthesized nanoparticles were characterized using powder X-ray diffraction, scanning electronic microscopy, and vibrating sample magnetometer analysis. The results showed that the microwave heating method produced smaller size nanoparticles with relatively narrower particle size distribution as well as stronger magnetic properties, compared with H-CF nanoparticles. The effect of photo-Fenton-like process parameters including UV light intensity (0–75 W), catalyst dosage (0–0.5 g/L), pH (2–5), hydrogen peroxide concentration (0–100 mmol/L), phenol initial concentration (20–500 mg/L), and temperature (35–55°C) on the phenol degradation was investigated. The kinetic data of phenol degradation using both synthesized nanoparticles were well fitted by pseudo-first-order kinetic model. The reaction times of phenol degradation over all ranges of phenol initial concentrations using M-CF catalyst were much smaller than those observed using H-CF catalyst. The obtained results indicated that the M-CF catalyst had a higher potential of phenol degradation compared with H-CF catalyst during photo-Fenton-like process.

Keywords: Phenol degradation; Photo-Fenton-like process; Cobalt ferrite nanoparticles; Microwave heating method; Conventional hydrothermal method; Operating parameters

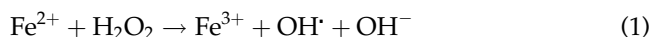
1. Introduction

Phenol is one of the hazardous materials and it is highly toxic to humans and environment at very low

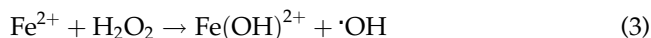
concentrations. The permissible limit of phenol is less than 0.5 mg/L in USEPA list [1]. Phenol is widely used in several industries including chemical, petrochemical, textile, food, and pharmaceuticals as a raw material [2]. So, the removal of phenol from wastes of those

*Corresponding authors.

industries is inevitable with respect to the environmental and public health issues [3]. Conventional methods including biological treatment, adsorption, and stripping are used to eliminate the phenol from the industrial wastes [4]. These techniques are associated with problems such as excessive time and lower efficiency [4]. However, advanced oxidation processes (AOPs) including Fenton [5], photo-Fenton [6], ozone oxidation [7], super critical oxidation [8], sonolysis [9], and photo-catalytic oxidation [10] are widely used for the treatment of phenol wastes. Among all, photo-Fenton process could be considered as an effective method. It could be attributed to its higher efficiency and more economical feasibility, compared to other AOPs [11,12]. Degradation of phenol in wastewater by AOPs is based on the generation of reactive free hydroxyl radicals ($\cdot\text{OH}$). It reacts with phenol by forming a double bond or by subtracting hydrogen atoms from organic molecules. In Fenton process, free hydroxyl radicals are generated from H_2O_2 in the presence of added Fe^{2+} ions as shown in the following equation [13]:



The degradation of phenol by Fenton process could be significantly accelerated in the presence of UV light irradiation (photo-Fenton process) [13,14]. It is because of Fe^{2+} ions formation upon photolysis of Fe^{3+} ions followed by reaction between Fe^{2+} and H_2O_2 to yield the hydroxyl radicals [Eqs. of (2) and (3)].



The spinel-structured ferrite nanoparticles with a general formula of MFe_2O_4 ($\text{M} = \text{Fe}, \text{Co}, \text{Cu}, \text{Mn}, \text{etc.}$), due to their unique physical and chemical properties, as well as magnetic properties, have been widely used in removing of organic compounds from aqueous systems [15–18]. Cobalt ferrite (CoFe_2O_4) nanoparticles, due to high magnetic anisotropy, high coercivity, mechanical hardness, chemical stability, moderate saturation magnetization, and magnetostriction, has been widely used for degradation of organic contaminants [19]. Several methods including hydrothermal, solvothermal, microwave, mechano-thermal, and seed-hydrothermal have been used for synthesis of spinel ferrite nanoparticles [20–22]. Among all, the microwave heating method has been rapidly developed as an alternative method due to rapid heating, faster

kinetics, homogeneity, higher yield, better reproducibility, and energy saving [23,24].

In the present study, cobalt ferrite nanoparticles were synthesized via microwave and conventional hydrothermal methods and the potential of synthesized nanoparticles was investigated for phenol degradation during photo-Fenton-like process. The influence of operating parameters including light intensity, catalyst dosage, pH, hydrogen peroxide concentration, phenol initial concentration, and temperature on the phenol degradation was investigated during photo-Fenton-like process.

2. Experimental

2.1. Materials and instruments

The chemical reagents were used containing $\text{FeSO}_4 \cdot 7\text{H}_2\text{O}$ (Sigma Aldrich, USA), $\text{CoCl}_2 \cdot 6\text{H}_2\text{O}$ (Sigma Aldrich, USA), NaOH (Merck, Darmstadt, Germany), Ethanol (Merck, Darmstadt, Germany), and phenol (analytical grade; Fluka).

The microwave equipment used in this study was a commercial microwave oven (CE1110 C, Sumsung, Korea) with 900 W output power at a wavelength of 2.45 GHz. The oven was equipped with an electronic system in order to control the temperature accurately.

2.2. Synthesis of cobalt ferrite nanoparticles

Cobalt ferrite nanoparticles were synthesized using both conventional and microwave heating methods. In both heating methods, firstly, 0.56 g of $\text{FeSO}_4 \cdot 7\text{H}_2\text{O}$ and 0.24 g of $\text{CoCl}_2 \cdot 6\text{H}_2\text{O}$ were dissolved in 20 mL of de-ionized water by intensive stirring to obtain the homogeneous solution. Then, NaOH was added to the solution and the stirring was continued at room temperature for 1 h. Since heating is known as a driving force of nanoparticles synthesis, the fundamental step in the synthesis is the application of conventional or microwave heating. Conventional hydrothermal method was conducted at 200°C for 5 h in a teflon-lined stainless-steel autoclave [25], whereas, the microwave heating method was applied at temperature of 160°C for 10 min. Then, the solid products were collected by magnetic filtration and washed by de-ionized water and ethanol. Finally, the samples were dried in a vacuum oven at 100°C for 6 h [26].

2.3. Measurement and methods

The powder's X-ray diffraction (XRD) patterns were recorded at 25°C on a Philips instrument (X'pert diffractometer using $\text{Cu-K}\alpha$ radiation) with a scanning speed of $0.03^\circ (2\theta) \text{ min}^{-1}$ to confirm the cobalt ferrite

nanoparticles structure. The morphology and particle size of nanoparticles were characterized using a scanning electron microscopy (SEM, TESCAN, VEGA 3SB). Magnetic characterization was conducted on a vibrating sample magnetometer (VSM, LDJ, 9600-1) at 300 K. Phenol concentrations were determined using a UV–vis spectrophotometer (JAS.CO V-530, Japan) at 271 nm.

2.4. Photo-Fenton-like process

The performance of the synthesized catalysts was evaluated in the photo-Fenton-like process of phenol degradation. Phenol degradation experiments were carried out under four UV lamps (one lamp intensity = 15 W, $\lambda_{\max} = 365$ nm) in a 500 mL pyrex-glass cell wrapped in aluminum foil. The schematic of photo-Fenton-like process is shown in Fig. 1. The effect of photo-Fenton-like parameters including UV light intensity (0–75 W), catalyst dosage (0–0.5 g/L), contact time (0–120 min), initial concentration of H_2O_2 (0–100 mM), pH (2–5), phenol initial concentration (20–500 mg/L), and temperature (35–55°C) were studied on the phenol degradation. Analysis was done using UV–vis spectroscopy at a maximum absorption peak of 271 nm. The degradation rate of phenol was calculated as follows:

$$D_e(\%) = \frac{(C_0 - C_t)}{C_0} \times 100\% \quad (4)$$

where D_e is the degradation rate of phenol after t min of reaction, C_t is the concentration of phenol after t min of reaction, and C_0 is the initial concentration of phenol.

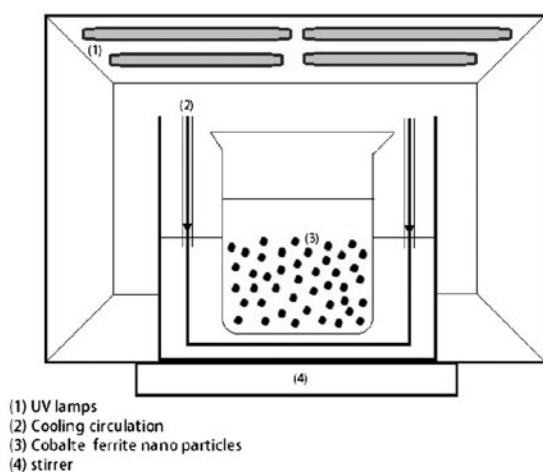


Fig. 1. Schematic of photo-Fenton-like process for phenol degradation.

3. Results

3.1. Characterization of cobalt ferrite nanoparticles

The X-diffraction patterns of synthesized cobalt ferrite nanoparticles by conventional (H-CF) and microwave heating methods (M-CF) are shown in Fig. 2. The diffraction of prepared nanoparticles using both of the methods indicated the expected peaks for the pure inverse spinel structure of CoFe_2O_4 (JCPDS 221086) [27]. Diffraction peaks of both nanoparticles revealed that no impurity was detected in the synthesized nanoparticles. Furthermore, diffraction peaks for M-CF nanoparticles was broader than those of another sample, indicating that the former sample consists of smaller crystallites compared with H-CF nanoparticles. The crystallite sizes (D) of nanoparticles were calculated from XRD peak broadening of the (3 1 1) peak using Scherrer formula: $D = 0.9\lambda/\beta \cos \theta$, where λ is the wavelength of $\text{CuK}\alpha$, β is the full width at half maxima of the diffraction peaks, and θ is the Bragg's angle. The crystallite sizes of H-CF and M-CF nanocatalysts were found to be about 26 and 14 nm, respectively.

Fig. 3 shows SEM images and particle size distribution of the CoFe_2O_4 nanocatalysts prepared by both techniques. As shown, the particle size of M-CF nanocatalyst was more uniform and smaller than that of H-CF nanocatalyst. The heat gradient in synthesis of M-CF catalyst may affect the more homogeneity in comparison to the H-CF catalyst synthesis. The rapid annealing of microwave sintering could retain the morphology, size, and shape of the nanoparticles during the densification of the particles which resulted in the smaller size of nanoparticles with sharper diameter distribution compared with H-CF nanoparticles. The average particle sizes of H-CF and M-CF nanoparticles

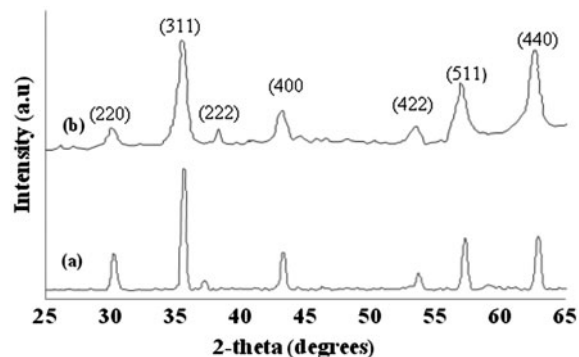


Fig. 2. XRD patterns of cobalt ferrite nanoparticles synthesized by (a) conventional hydrothermal and (b) microwave heating methods.

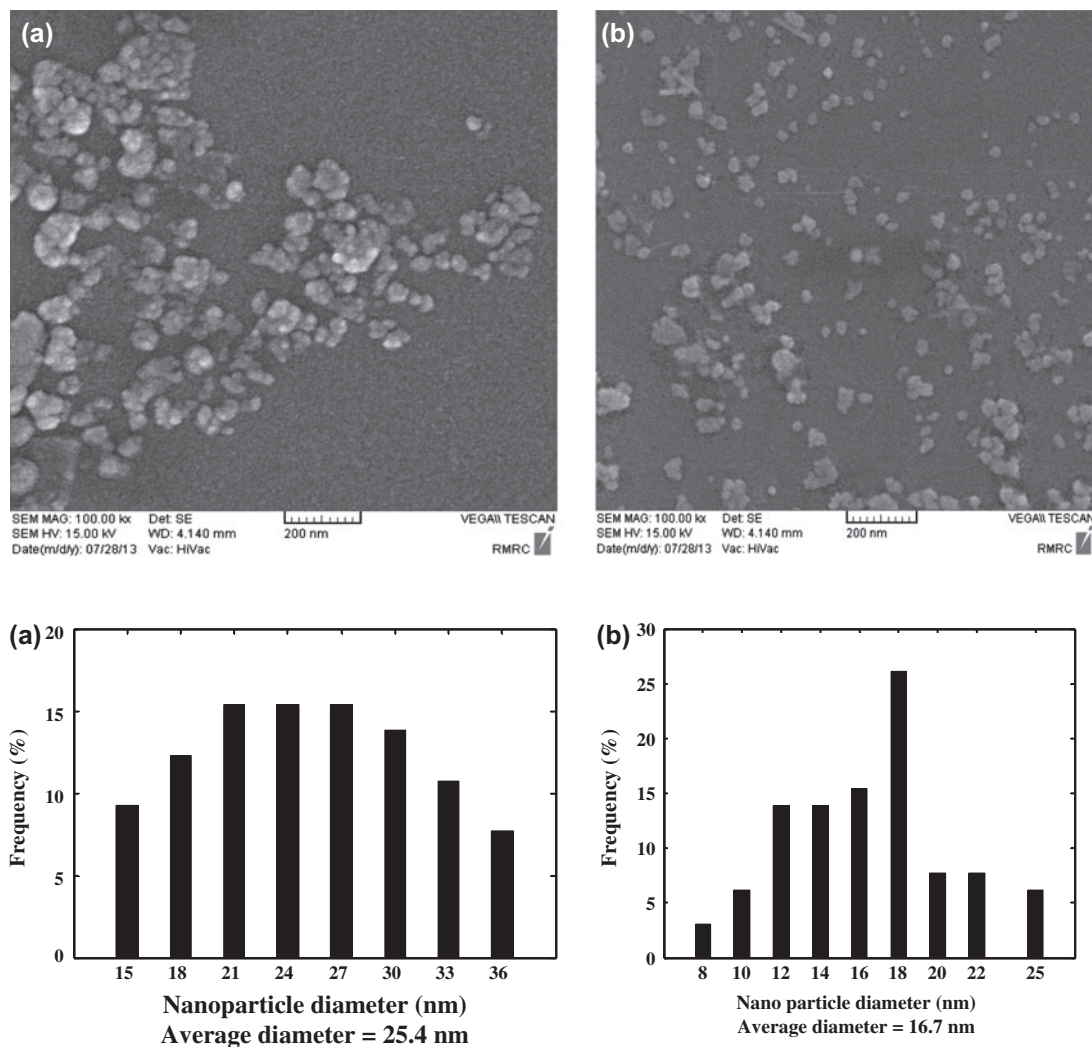


Fig. 3. SEM images and particle size distribution of cobalt ferrite nanoparticles prepared by (a) hydrothermal and (b) microwave methods.

were found to be 25.4 and 16.7 nm which was in good agreement with the crystallite sizes calculated by the XRD patterns.

The magnetic properties of the H-CF and M-CF nanoparticles are investigated which results are shown in Fig. 4 and summarized in Table 1. The magnetic properties of the nanosized materials depend on the preparation method as well as the crystallite size [28]. As shown, the coercivity (H_c) of nanoparticles prepared by microwave and hydrothermal techniques were found to be 833.7 and 642.5, respectively. It could be due to the smaller size and more uniform of samples prepared using microwave heating method in comparison to sample prepared by conventional heating method. Similar trends are presented by other researchers [29,30]. The saturation magnetization (M_s)

of sample decreases commonly if the particle size decreases to the nanoscale due to the disorder canting spins on the surfaces [30]. However, the obtained saturation magnetization of M-CF nanocatalyst (92.5 emu/g) was more than H-CF catalyst (66.5 emu/g). This behavior could be attributed to the presence of undetectable very small clusters of metallic Co(0) and/or Fe(0) [31].

3.2. Effect of light intensity on the phenol degradation

To study the influence of different light intensity on the degradation of phenol during photo-Fenton-like process, the system was equipped with UV lamps. A number of experiments were carried out, applying various light intensities generated from 0, 1, 2, 3, 4,

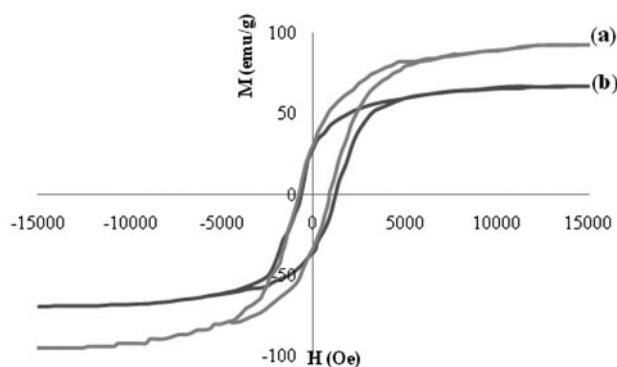


Fig. 4. Hysteresis loops of synthesized cobalt ferrite nanoparticles by (a) microwave and (b) hydrothermal methods.

Table 1
Magnetic properties of the cobalt ferrite nanoparticles

Catalyst	M_s (emu/g)	M_r (emu/g)	H_c (Oe)
H-CF	66.5	31.35	833.7
M-CF	92.5	28.65	642.5

and 5 lamps. The results of phenol degradation percentage for initial phenol concentration of 100 mg/L, hydrogen peroxide concentration of 30 M, catalyst dosage of 0.3 g/L, pH of 3, and temperature of 35°C after 2 h reaction time are shown in Fig. 5. As shown, the phenol degradation percentages were increased by increasing the light intensity up to 60 W (four lamps of 15 W) for both synthesized nanoparticles. After that, the phenol degradation did not change remarkably by increasing the light intensity. Therefore, the light intensity of 60 W is selected for further experiments.

3.3. Effect of catalyst dosage on phenol degradation

The effect of cobalt ferrite dosage synthesized using hydrothermal and microwave heating methods on the phenol degradation for initial phenol concentration of 100 mg/L, hydrogen peroxide concentration of 30 M, pH of 3, and temperature of 35°C after 1 and 2 h contact time are presented in Fig. 6. As shown in Fig. 6(a), the degradation rate of phenol increased by increasing the catalyst dosage up to 0.3 g/L after 1 and 2 h contact time for cobalt ferrite nanoparticles synthesized by hydrothermal method (H-CF). Fig. 6(b) showed that the optimal loading of cobalt ferrite nanoparticles synthesized by microwave heating method (M-CF) catalyst for the maximum phenol degradation rate was found to be 0.2 g/L in 2 h contact time and 0.3 g/L in 1 h reaction time. Further increase in the

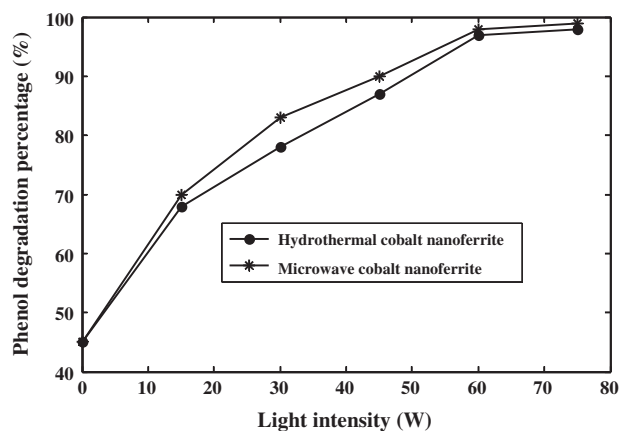


Fig. 5. Effect of light intensity on the phenol degradation for initial phenol concentration of 100 mg/L, hydrogen peroxide concentration of 30 M, catalyst dosage of 0.3 g/L, pH of 3, and temperature of 35°C after 2 h reaction time.

catalyst dosage to 0.5 g/L resulted in a reduction of phenol degradation rate for both of the synthesized nanoparticles. As shown, the required catalyst dosages for the complete degradation of phenol were found to be 0.2 and 0.3 g/L using M-CF and H-CF nanoparticles after 2 h reaction time. It could be attributed to the smaller size and stronger magnetic properties of M-CF nanoparticles compared with H-CF nanoparticles which resulted in complete degradation of phenol in lower catalyst dosages. Increase in phenol degradation rate by increasing of catalyst dosage up to 0.3 g/L for both synthesized nanoparticles could be attributed to the increase in catalyst active surface for phenol degradation. Reduction of phenol degradation rate in higher catalyst dosages than 0.3 g/L for both H-CF and M-CF could be attributed to the agglomeration of catalyst particles which decreased the number of active sites on the catalyst surface for reaction with phenol molecules. Furthermore, the excessive catalyst loading increased the turbidity of the solution and consequently, decreased the light penetration through the solution which resulted in the decrease in active surface of catalyst for light harvesting and reduction in the catalyst efficacy for phenol degradation. Similar trends are reported by other researchers [10,32]. More reduction of phenol degradation gradient for higher catalyst dosages than 0.3 g/L and contact time of 2 h compared with 1 h for both synthesized nanoparticles may be attributed to the agglomeration and coagulation of nanoparticles which decreased the ability of nanoparticles in degradation of phenol during photo-Fenton-like process. Furthermore, 0.3 g/L of catalyst dosages of both synthesized nanoparticles is selected

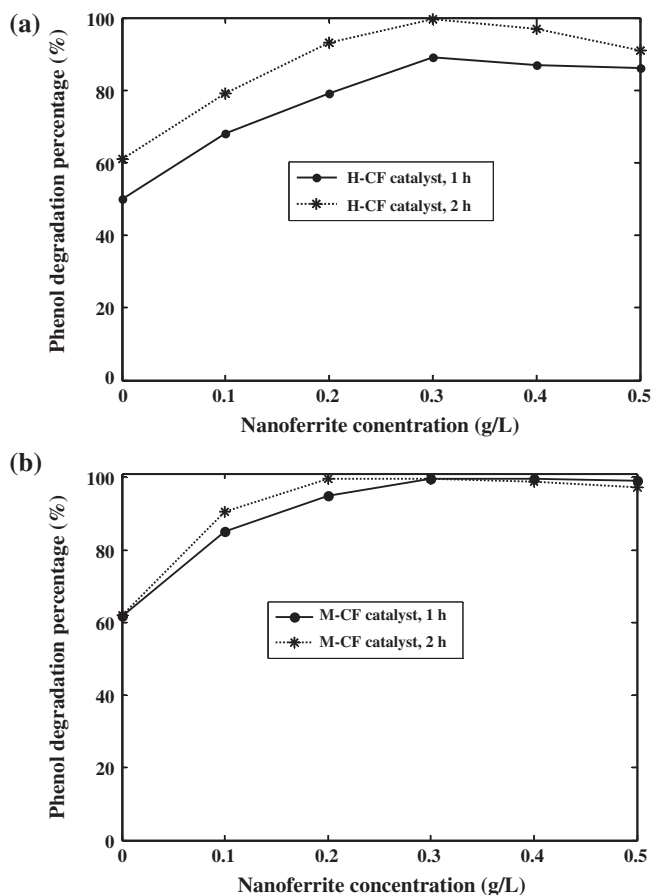


Fig. 6. Effect of cobalt ferrite dosage synthesized by (a) hydrothermal method and (b) microwave methods on the phenol degradation rate for initial phenol concentration of 100 mg/L, hydrogen peroxide concentration of 30 M, pH of 3, and temperature of 35°C after 1 and 2 h reaction time.

as an optimum value for further experiments of phenol degradation.

3.4. Effect of hydrogen peroxide concentration on the phenol degradation

Hydroxyl radicals play an important role in the organic contaminants degradation. Generating more radicals accelerate the degradation efficiency. By addition of hydrogen peroxide (HP) into the solution, the concentration of hydroxyl radicals increases which can lead to an enhancement in the rate of phenol degradation. The effect of HP concentration on the phenol degradation rate using synthesized cobalt ferrite nanoparticles in the phenol initial concentration of 100 mg/L, pH of 3, and temperature of 35°C after 1 h

contact time is shown in Fig. 7. As shown, phenol degradation rate increased by increasing of HP concentration amount up to 50 mmol/L. Further increase in the HP concentration led to decrease in the phenol degradation rate using both of synthesized nanoparticles. The enhancement of phenol degradation rate by increasing of HP concentration could be due to the increase in hydroxyl radical concentration through the reaction. Reduction in the phenol degradation rates in HP concentrations higher than 50 mmol/L could be attributed to quenching of $\cdot\text{OH}$ radicals by excessive HP to form a less active HO_2 (1.7 eV) compared with the $\cdot\text{OH}$ radical (2.8 eV). Since, the difference of the phenol degradation rates using 30, 40, and 50 mmol/L of HP concentrations is low; it is economical to use 30 mmol/L of HP concentration for phenol degradation. Consequently, the optimum concentration of HP is selected as 30 mmol/L for further experiments.

3.5. Effect of pH on the phenol degradation

The pH of the solution has a major role in the degradation of organic pollutants. The influence of pH on the phenol degradation rate using of both H-CF and M-CF catalysts in the pH range of 2–5 for the phenol concentration of 100 mg/L, catalyst dosage of 0.3 g/L, HP concentration of 30 mM, and temperature of 35°C after 1 h contact time is presented in Fig. 8. As shown, the phenol degradation rate reached a maximum value at pH of 3.0. The lower degradation rate of phenol at lower pH values than 3 could be due to $\text{OH}\cdot$ scavenging by H^+ ions ($\text{OH}\cdot + \text{H}^+ + \text{Fe}^{2+} \rightarrow \text{H}_2\text{O} + \text{Fe}^{3+}$). Furthermore, at lower pH values, the

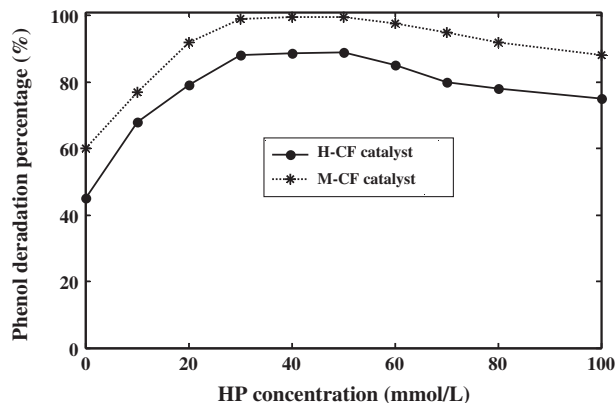


Fig. 7. Effect of hydrogen peroxide concentration on the phenol degradation using H-CF and M-CF catalysts after 1 h contact time for phenol concentration of 100 mg/L, pH of 3, and temperature of 35°C.

reaction was slowed due to the formation of complexes of $[\text{Fe}(\text{H}_2\text{O})_6]^{2+}$, which reacted more slowly with hydrogen peroxide in comparison to reaction rate of $[\text{Fe}(\text{OH})(\text{H}_2\text{O})_5]^{2+}$ which led to reduction of phenol degradation efficiency. Reduction in the phenol degradation rate in the pH values more than 3, could be attributed to the decrease in the oxidation potential of $\cdot\text{OH}$ with an increase in pH values. Therefore, the pH of 3 is selected as an optimum value for further experiments of phenol degradation.

3.6. Effect of phenol initial concentration on the phenol degradation

The effect of phenol initial concentration on the degradation of phenol, using both synthesized nanoparticles in the catalyst dosage of 0.3 g/L, H_2O_2 concentration of 30 mM, pH of 3, and temperature of 35°C are shown in Fig. 9. The results indicated that the irradiation time required for complete degradation of phenol using both synthesized nanoparticles increased by increasing the initial phenol concentration. Furthermore, at higher concentrations than 100 mg/L using H-CF catalyst as well as higher concentrations than 200 mg/L using M-CF catalyst, the complete degradation of phenol, due to the limited number of requirement of reactive species ($\cdot\text{OH}$ and $\cdot\text{O}_2$) needed for the complete degradation of phenol, was impossible. Also, the higher degradation rate of phenol using M-CF catalyst comparing with H-CF catalyst could be attributed to higher specific area, smaller size, and more homogeneity of M-CF catalyst

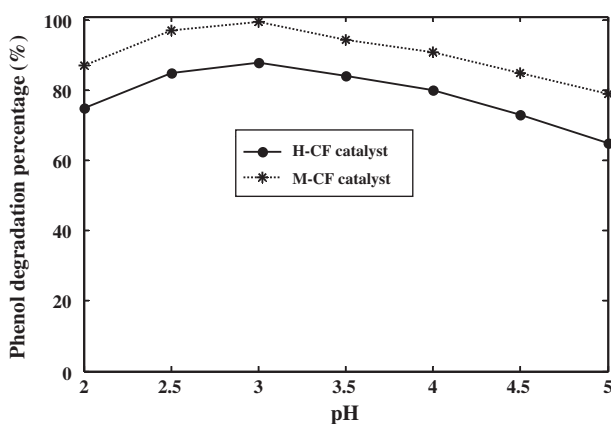


Fig. 8. Effect of pH on the phenol degradation rate using of both H-CF and M-CF catalysts for initial phenol concentration of 100 mg/L, catalyst dosage of 0.3 g/L, H_2O_2 concentration of 30 mmol/L, contact time of 1 h, and temperature of 35°C.

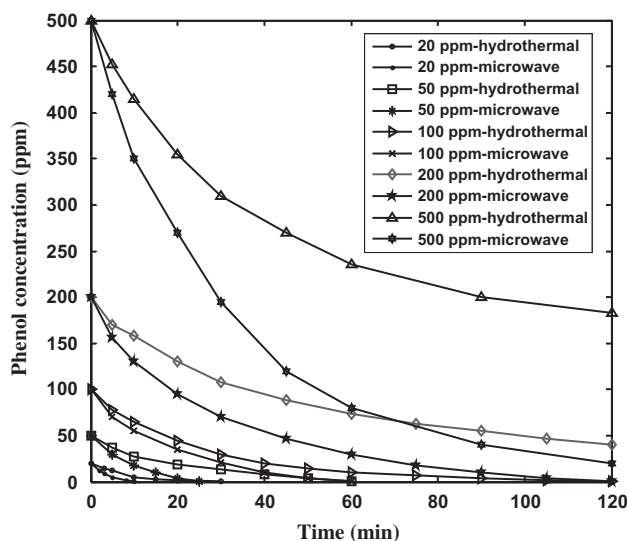


Fig. 9. Effect of phenol initial concentration on the degradation of phenol, using both synthesized nanoparticles in the catalyst dosage of 0.3 g/L, H_2O_2 concentration of 30 mmol/L, pH of 3, and temperature of 35°C.

nanoparticles comparing with H-CF catalyst nanoparticles, which resulted in the more number of available sites of M-CF catalyst and, consequently, in the higher catalytic activity of M-CF catalyst for phenol degradation compared with H-CF catalyst.

3.7. Effect of temperature on the phenol degradation

The effect of temperature on the phenol degradation using both synthesized cobalt ferrite nanoparticles for 500 mg/L of phenol concentration, catalyst dosage of 0.3 g/L, H_2O_2 concentration of 30 mM, and pH of 3 are shown in Fig. 10. As shown, the phenol degradation rate increased with the increasing of temperature amount up to 45°C. Further increase in temperature amounts led to decrease in phenol degradation using both synthesized nanoparticles. When the reaction temperature increased, the rate of hydroxylation at the catalyst active sites produced more $\cdot\text{OH}$ free radicals resulted in higher collision between the $\cdot\text{OH}$ radicals and the phenol molecules and consequently, increase in phenol degradation rate. Decreasing of phenol degradation rate in temperature higher than 45°C could be attributed to the thermal decomposition of hydrogen peroxide ($\text{H}_2\text{O}_2 \rightarrow \text{H}_2\text{O} + \text{O}_2$) which resulted in scavenging of $\cdot\text{OH}$ radicals and decreasing of phenol degradation rate which were not investigated in this work. Similar trends are reported by other researchers [33,34].

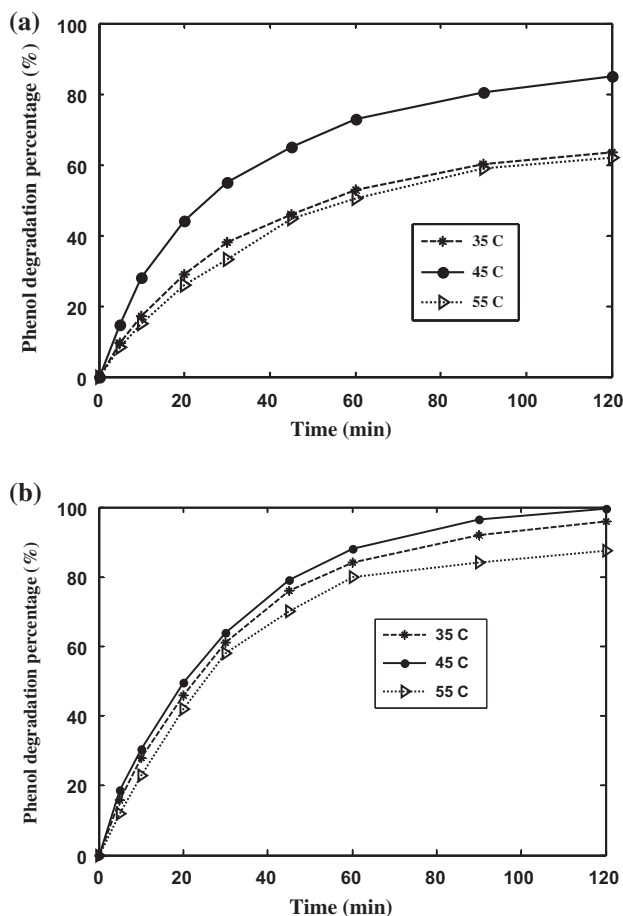


Fig. 10. Effect of temperature on the phenol degradation using both synthesized cobalt ferrite nanoparticles for 500 mg/L of phenol concentration, catalyst dosage of 0.3 g/L, H_2O_2 concentration of 30 mmol/L, pH of 3, and temperature of 35°C.

3.8 Kinetic and half time reaction

The Langmuir–Hinshelwood model is usually used to describe the degradation of organic pollutants in aqueous suspension. This model is expressed as follows:

$$r = \frac{-dc}{dt} = \frac{k_r k_a C}{1 + k_a C} \quad (5)$$

where r is the reaction rate, k_r is the reaction rate constant, k_a is the absorption coefficient of the reactant, and C is the reactant concentration. When the reactant concentration is low, Eq. (5) can be described as first-order kinetic model.

$$r = \frac{-dc}{dt} = kC \quad (6)$$

where k is the first-order rate constant. Set $t = 0$, $C = C_0$, Eq. (7) could be induced.

$$C = C_0 \exp(-k_{app}t) \quad (7)$$

where C_0 is the initial concentration of the pollutant. The constant of the first-order kinetic model was calculated by plotting C vs. t at different concentrations of phenol (20, 50, and 100 mg/L) using both of synthesized nanoparticles, the results of which are presented in Table 2. The higher values of correlation coefficient (R^2) than 0.99 confirmed that the first-order kinetic model was well described, the kinetic data of phenol degradation.

For the reaction with the first-order kinetic model, the half-life time can be calculated as follows:

$$t_{1/2} = \frac{\ln 2}{k_{app}} \quad (8)$$

where $t_{1/2}$ is the half-life time reaction of phenol degradation. The results of which are also presented in Table 2. As shown, the half-life times reaction ($t_{1/2}$) of phenol degradation over all ranges of phenol initial concentrations (20–100 mg/L) using M-CF catalyst were much smaller than those observed using H-CF catalyst. These results indicated the higher potentiality of M-CF catalyst compared with H-CF catalyst for phenol degradation.

Table 2

First-order constants, half-life times, and regression coefficients of phenol degradation at different phenol initial concentrations using synthesized cobalt ferrite nanoparticles

Catalyst	First-order rate constant (k_{app})						Half-life time ($t_{0.5}$)		
	20 ppm	R^2	50 ppm	R^2	100 ppm	R^2	20 ppm	50 ppm	100 ppm
H-CF	0.1205	0.990	0.0512	0.990	0.0401	0.997	5.75	13.54	17.29
M-CF	0.2769	0.993	0.1089	0.994	0.0574	0.994	2.50	6.36	12.08

4. Conclusion

Photo-Fenton catalysts of magnetic cobalt ferrite nanoparticles were successfully synthesized by the conventional hydrothermal method (H-CF) and microwave heating method (M-CF). The potential of the synthesized nanoparticles for degradation of phenol was investigated. The XRD patterns of nanoparticles revealed the formation of single phase of cobalt ferrite synthesized using both methods. The SEM images of nanoparticles indicated that the particle size of M-CF catalyst was more uniform and smaller than that of H-CF catalyst. The VSM analysis of nanoparticles confirmed the stronger magnetic properties of M-CF catalyst compared with H-CF catalyst. The experimental results of phenol degradation in photo-Fenton-like process indicated that the optimal conditions for maximum phenol degradation using both synthesized nanoparticles were found to have light intensity of 60 W, catalyst dosage of 0.3 g/L, pH of 3, hydrogen peroxide concentration of 30 mmol/L, and temperature of 45°C. Kinetic studies showed that the phenol degradation onto the M-CF and H-CF catalysts, followed the first-order reaction. The results of reaction time effect on the phenol degradation during photo-Fenton-like process revealed that the required time for complete phenol degradation using M-CF catalyst was much shorter compared with H-CF catalyst. The obtained results of which exhibited the better activity of M-CF catalyst for phenol degradation compared with H-CF catalyst.

References

- [1] F. Adam, J. Andas, I.Ab. Rahman, A study on the oxidation of phenol by heterogeneous iron silica catalyst, *Chem. Eng. J.* 165 (2010) 658–667.
- [2] O.B. Ayodele, J.K. Lim, B.H. Hameed, Degradation of phenol in photo-Fenton process by phosphoric acid modified kaolin supported ferric-oxalate catalyst: Optimization and kinetic modeling, *Chem. Eng. J.* 197 (2012) 181–192.
- [3] S. Ahmed, M.G. Rasul, W.N. Martens, R. Brown, M.A. Hashib, Heterogeneous photocatalytic degradation of phenols in wastewater: A review on current status and developments, *Desalination* 261 (2010) 3–18.
- [4] B. Iurascu, I. Siminiceanu, D. Vione, M.A. Vicente, A. Gil, Phenol degradation in water through a heterogeneous photo-Fenton process catalyzed by Fe-treated laponite, *Water Res.* 43 (2009) 1313–1322.
- [5] R.F.F. Pontes, J.E.F. Moraes, A. Machulek Jr., J.M. Pinto, A mechanistic kinetic model for phenol degradation by the Fenton process, *J. Hazard. Mater.* 176 (2010) 402–413.
- [6] R.R. Navarro, H. Ichikawa, K. Tatsumi, Ferrite formation from photo-Fenton treated wastewater, *Chemosphere* 80 (2010) 404–409.
- [7] O. Legrini, E. Oliveros, A.M. Braun, Photochemical processes for water treatment, *Chem. Rev.* 93 (1993) 671–698.
- [8] I. Vera Pérez, S. Rogak, R. Branion, Supercritical water oxidation of phenol and 2,4-dinitrophenol, *J. Supercrit. Fluids* 30 (2004) 71–87.
- [9] A. Babuponnusami, K. Muthukumar, Degradation of phenol in aqueous solution by Fenton, sono-Fenton and sono-photo-Fenton methods, *J. Clean Soil Air Water* 39 (2011) 142–147.
- [10] C.Mc. Manamon, J.D. Holmes, M.A. Morris, Improved photocatalytic degradation rates of phenol achieved using novel porous ZrO₂-doped TiO₂ nanoparticulate powders, *J. Hazard. Mater.* 193 (2011) 120–127.
- [11] G. Zelmanov, R. Semiat, Iron(3) oxide-based nanoparticles as catalysts in advanced organic aqueous oxidation, *Water Res.* 42 (2008) 492–498.
- [12] S.Q. Liu, L.R. Feng, N. Xu, Z.G. Chen, X.M. Wang, Magnetic nickel ferrite as a heterogeneous photo-Fenton catalyst for the degradation of rhodamine B in the presence of oxalic acid, *Chem. Eng. J.* 203 (2012) 432–439.
- [13] R.G. Zepp, B.C. Faust, J. Hoigne, Hydroxyl radical formation in aqueous reactions (pH 3–8) of iron(II) with hydrogen peroxide: The photo-Fenton reaction, *J. Environ. Sci. Technol.* 26 (1992) 313–319.
- [14] A. Safarzadeh-Amiri, J.R. Bolton, S.R. Cater, Ferrioxalate-mediated photodegradation of organic pollutants in contaminated water, *Water Res.* 31 (1997) 787–798.
- [15] D. Guin, B. Baruwati, S.V. Manorama, A simple chemical synthesis of nanocrystalline AFe₂O₄ (A=Fe, Ni, Zn): An efficient catalyst for selective oxidation of styrene, *J. Mol. Catal. A Chem.* 242 (2005) 26–31.
- [16] S. Zhang, H. Niu, Y. Cai, X. Zhao, Y. Shi, Arsenite and arsenate adsorption on coprecipitated bimetal oxide magnetic nanomaterials. MnFe₂O₄ and CoFe₂O₄, *Chem. Eng. J.* 158 (2010) 599–607.
- [17] P. Baldrian, V. Merhautová, J. Gabriel, F. Nerud, P. Stopka, M. Hrubý, M.J. Beneš, Decolorization of synthetic dyes by hydrogen peroxide with heterogeneous catalysis by mixed iron oxides, *Appl. Catal., B* 66 (2006) 258–264.
- [18] L. Zhao, X. Li, Q. Zhao, Z. Qu, D. Yuan, S. Liu, X. Hu, G. Chen, Synthesis, characterization and adsorptive performance of MgFe₂O₄ nanospheres for SO₂ removal, *J. Hazard. Mater.* 184 (2010) 704–709.
- [19] E. Manova, T. Tsoncheva, D. Paneva, I. Mitov, K. Tenchev, L. Petrov, Mechanochemically synthesized nano-dimensional iron–cobalt spinel oxides as catalysts for methanol decomposition, *Appl. Catal., A* 277 (2004) 119–127.
- [20] S.D. Shenoy, P.A. Joy, M.R. Anantharaman, Effect of mechanical milling on the structural, magnetic and dielectric properties of coprecipitated ultrafine zinc ferrite, *J. Magn. Magn. Mater.* 269 (2004) 217–226.
- [21] H.H. Hamdeh, J.C. Ho, S.A. Oliver, R.J. Willey, G. Oliveri, G.J. Busca, Magnetic properties of partially-inverted zinc ferrite aerogel powders, *J. Appl. Phys.* 81 (1997) 1851–1857.
- [22] S.H. Yu, T. Fujino, M. Yoshimura, Hydrothermal synthesis of ZnFe₂O₄ ultrafine particles with high magnetization, *J. Magn. Magn. Mater.* 256 (2003) 420–424.

- [23] X.L. Hu, J.C. Yu, J.M. Gong, Q. Li, G.S. Li, Alpha- Fe_2O_3 nanorings prepared by a microwave-assisted hydrothermal process and their sensing properties, *Adv. Mater.* 19 (2007) 2324–2329.
- [24] S-W. Cao, Y.-J. Zhu, G.-F. Cheng, Y.-H. Huang, ZnFe_2O_4 nanoparticles: Microwave-hydrothermal ionic liquid synthesis and photocatalytic property over phenol, *J. Hazard. Mater.* 171 (2009) 431–435.
- [25] L. Wang, J. Li, Y. Wang, L. Zhao, Q. Jiang, Adsorption capability for Congo red on nanocrystalline MFe_2O_4 ($\text{M} = \text{Mn}, \text{Fe}, \text{Co}, \text{Ni}$) spinel ferrites, *Chem. Eng. J.* 182 (2012) 72–79.
- [26] J. Xia, A. Wang, X. Liu, Z. Su, Preparation and characterization of bifunctional, $\text{Fe}_3\text{O}_4/\text{ZnO}$ nanocomposites and their use as photocatalysts, *Appl. Surf. Sci.* 257 (2011) 9724–9732.
- [27] M. Goodarz Naseri, E. Saion, H. Abbastabar Ahangar, H. Shaari, M. Hashim, Simple synthesis and characterization of cobalt ferrite nanoparticles by a thermal treatment method, *J. Nanomater.* 1 (2010) 1–8.
- [28] A.M. Ibrahim, M.M. El-Latif, M.M. Mahmoud, Synthesis and characterization of nano-sized cobalt ferrite prepared via polyol method using conventional and microwave heating techniques, *J. Alloys. Comp.* 506 (2010) 201–204.
- [29] T. Caillot, G. Pourroy, D. Stuerge, Microwave hydrothermal flash synthesis of nanocomposites Fe–Co alloy/cobalt ferrite, *J. Solid State Chem.* 177 (2004) 3843–3848.
- [30] I.H. Gul, A. Maqsood, Structural, magnetic and electrical properties of cobalt ferrites prepared by the sol-gel route, *J. Alloys. Comp.* 465 (2008) 227–231.
- [31] D. Michael, P. Mingos, D.R. Baghurst, Application of microwave dielectric heating effects to synthetic problems in chemistry, *Chem. Soc. Rev.* 20 (1991) 1–47.
- [32] Y.A. Shaban, M.A. El Sayed, A.A. El Maradny, R.K. Al Farawati, M.I. Al Zobidi, Photocatalytic degradation of phenol in natural seawater using visible light active carbon modified (CM)- n-TiO_2 nanoparticles under UV light and natural sunlight illuminations, *Chemosphere* 91 (2013) 307–313.
- [33] A.C.K. Yip, F.L.Y. Lam, X. Hu, Chemical-vapor-deposited copper on acid-activated bentonite clay as an applicable heterogeneous catalyst for the photo-Fenton-like oxidation of textile organic pollutants. *Ind. Eng. Chem. Res.* 44 (2005) 7983–7990.
- [34] B. Muthukumari, K. Selvam, I. Muthuvel, M. Swaminathan, Photoassisted hetero-Fenton mineralisation of azo dyes by $\text{Fe(II)-Al}_2\text{O}_3$ catalyst, *Chem. Eng. J.* 153 (2009) 9–15.